# Magnetic circular dichroism in X-ray emission

Advanced hard and soft magnets are key devices in modern technologies and are widely used in our everyday lives. Permanent magnets with high flux density and high coercivity are used in the motors in electric vehicles; electrical steel with high permeability and low core loss is used in transformers that supply electricity to houses. In order to improve the magnetic properties of these materials, it is necessary to observe the spatial distribution of magnetic domains under static and oscillating magnetic fields. In particular, observation of magnetic domains well below the surface of bulk magnetic materials is required from the viewpoint of industrial applications.

X-ray magnetic circular dichroism in the hard X-ray region (HXMCD) is a powerful technique suitable for the above-mentioned purpose. It utilizes a phenomenon that the X-ray absorption cross section of magnetized materials depends on whether the magnetization and the helicity of circularly polarized incident X-rays are parallel or antiparallel, particularly near the absorption edges. The use of highly collimated synchrotron X-rays in HXMCD makes it possible to provide a moderate spatial resolution of a few hundreds nanometers without a large loss of incident flux. The attenuation length of X-rays ranging from 5 to 10 keV, at which the *K* absorption edges of 3*d* transition-metal (TM) elements and *L* absorption edges of rare-earth elements reside, is approximately on the order of 10 μm. Accordingly, bulk-sensitive and element-selective magnetic microscopy is realized using HXMCD [1].

However, a disadvantage of HXMCD is a very small dichroic effect (about 0.5%) for 3*d* TMs, such as Fe, Co, and Ni, despite the fact that they are crucial elements in ferromagnetic materials. This difficulty has been overcome by using phase-sensitive detection for thin films [2], whereas it is still a problem for measurements of bulk materials. Therefore, there has been strong demand to find a new principle that enables magnetic circular dichroism measurement to be performed with a large dichroic effect for 3*d* TMs in the hard X-ray region. In this research, a new magneto-optical effect in the X-ray region is proposed and experimentally confirmed [3]. The new effect is that the dichroic effect is exhibited in X-ray emission, in sharp contrast to conventional XMCD, in which the dichroic effect is observed in X-ray absorption.

The basic idea of the new magneto-optical effect is presented below and also illustrated in Fig. 1. A spin-orbit coupling is a key requisite in magnetic circular dichroism. For instance, a small dichroic effect at the *K* absorption process of 3*d* TMs ($1s \rightarrow 4p$) stems from the fact that there is no large effective spin-orbit coupling in both 1*s* and 4*p* orbitals. In contrast, a large spin-orbit coupling exists in the final $2p^5$ state in the $K\alpha$ emission process ($2p \rightarrow 1s$). The $2p^5$ state splits into a $2p_{1/2}$ doublet and a $2p_{3/2}$ quartet owing to the large spin-orbit coupling, where the $2p_{3/2} \rightarrow 1s$ transition corresponds to the $K\alpha_1$ emission. The $2p_{3/2}$ quartet further splits because of the spin polarization in the 3*d* orbital through the sizable 2*p*3*d* exchange interaction. The resulting spin splitting of the $2p_{3/2}$ quartet also produces orbital splitting since the orbital state tightly couples to the spin state. Accordingly, because of this orbital splitting, a large dichroic effect is expected in the $K\alpha_1$ emission of 3*d* TMs.

The validity of this idea was established in experiments at SPring-8 **BL22XU**. The experimental setup is introduced below in detail and is illustrated in Fig. 2. The sample was an iron single crystal, which was inserted between permanent magnets in order to saturate the magnetization. The sample was illuminated by intense incident X-rays generated from an undulator and emitted fluorescence X-rays, which were collimated by an exit slit down to a divergence of 120 μrad in order that the optical elements mentioned below could operate. The quarter-wave plate (QWP)

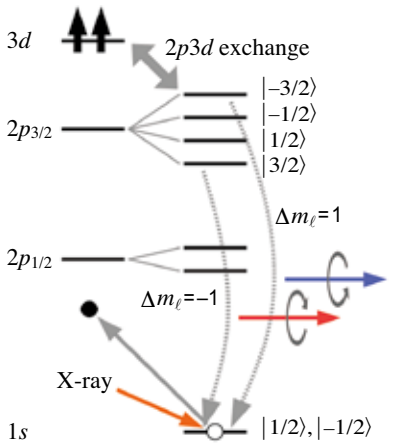


Fig. 1. $K\alpha_1$ emission process of a 3*d* TM ferromagnet. A 1*s* electron is promoted by an incident photon, and then a 2*p* electron fills the 1*s* core hole, emitting a $K\alpha$ photon. Representative two transitions are shown. The final $2p^5$ state splits into a $2p_{3/2}$ quartet and a $2p_{1/2}$ doublet owing to a spin-orbit coupling and further splits owing to a 2*p*3*d* exchange interaction. Numbers are the magnetic quantum numbers of sublevels and $\Delta m_\ell$ is the change in the orbital magnetic quantum number at the transition.

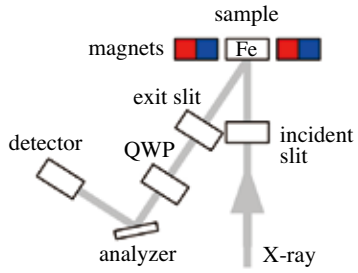


Fig. 2. Top view of the experimental layout. QWP: diamond phase retarder that acts as a quarter-wave plate. Analyzer: Ge(400) single crystal that is used as both an energy and polarization analyzer.

was a diamond single crystal and is a device that mutually converts circularly polarized X-rays and linearly polarized X-rays. The polarization analyzer that reflected the vertical component of the incoming fluorescence X-rays was a Ge single crystal and also functioned as an energy analyzer. The combination of a QWP and a polarization analyzer is a standard device for detecting the circular polarization of a beam of photons. In short, the device transmits right (left) circularly polarized X-rays and 50% linearly polarized X-rays when the QWP generates a $\pi/2$ ($-\pi/2$) phase shift.

The obtained Fe $K\alpha_1$ emission spectra are indicated in Fig. 3(a). $I^+$ (red open circles) and $I^-$ (blue closed circles) are data observed when the $\pi/2$ and $-\pi/2$ phase shifts are induced by the QWP, respectively. The magnetic field is applied as shown in the inset (positive direction). It is clear that the $I^+$ spectrum is shifted to the low-energy side by about 0.3 eV compared with the $I^-$ spectrum. The difference between the two spectra is direct evidence that the $K\alpha_1$ emission is circularly polarized. When the magnetic field is reversed, the tendency is reversed as shown in Fig. 3(b). The difference spectra $I^+-I^-$ normalized by the peak intensity of the sum of the spectra are also shown in Fig. 3(c).

These results clearly illustrate that (i) the energy-resolved $K\alpha_1$ spectrum of ferromagnetic Fe indicates finite circular polarization and (ii) the circular polarization is inverted when the magnetization of the sample is inverted. These two features unambiguously indicate the existence of XMCD in the Fe $K\alpha_1$ emission. The flipping ratio $(I^+-I^-)/(I^++I^-)$ is a measure of the size of the dichroic effect and was 12 ± 4% at 6.405 keV. If the corrections for the scattering angle and the efficiency of the QWP are taken into account, the value would amount to 18 ± 6%.

To summarize, it was experimentally confirmed that magnetic circular dichroism actually exists in X-ray core-level emission and that the dichroic effect is quite large even in the *K*-edge of 3*d* TMs. Hence, this magneto-optical effect may open a new way to perform element-selective and truly bulk-sensitive measurements of the magnetization of 3*d* TMs.

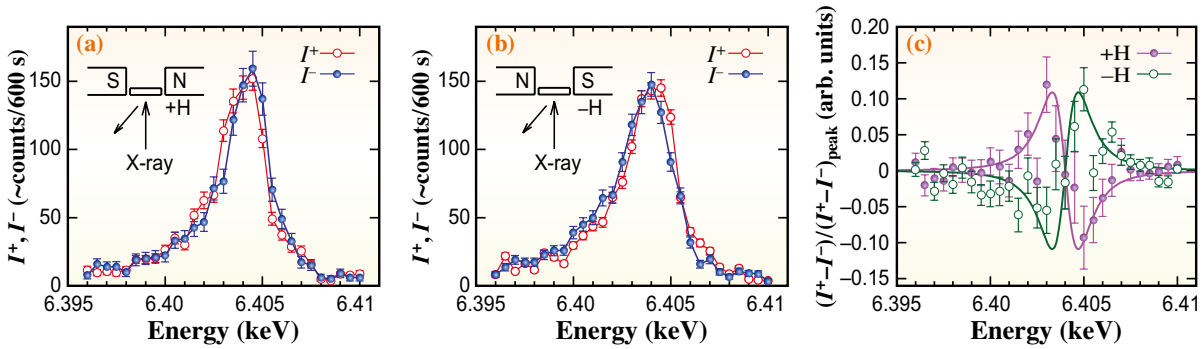


Fig. 3. **(a)** Fe $K\alpha_1$ emission spectra $I^+$ and $I^-$ for a phase shift of $\pi/2$ (red open circles) and $-\pi/2$ (blue solid circles), respectively. The lines connect the data points to guide the eye. The magnetic field is applied as shown in the inset and the direction is defined as positive. The $I^+$ spectrum is shifted to the low energy side compared with the $I^-$ spectrum. **(b)** Fe $K\alpha_1$ emission spectra $I^+$ and $I^-$ when the magnetic field is applied along the negative direction. In contrast to (a), the $I^+$ spectrum is shifted to the high energy side. **(c)** Difference spectra between $I^+$ and $I^-$ normalized by the peak intensity of the sum of the spectra. Magenta solid circles and green open circles are measurements when the magnetic field is directed along the positive and negative directions, respectively. Solid lines are a guide to the eye.

Toshiya Inami

National Institutes for Quantum and Radiological Science and Technology (QST)

Email: inami.toshiya@qst.go.jp

**References**

[1] M. Suzuki *et al.*: Acta Mater. **106** (2016) 155.
[2] T. Nakamura and M. Suzuki: J. Phys. Soc. Jpn. **82** (2013) 021006.
[3] *T. Inami: Phys. Rev. Lett.* ***119*** *(2017) 137203.*